

Reprinted from The Journal of Physical Chemistry, 1995, 99.  
Copyright © 1995 by the American Chemical Society and reprinted by permission of the copyright owner.

## Differentiating Functional Groups with the Scanning Tunneling Microscope

Bhawani Venkataraman and George W. Flynn\*

Department of Chemistry and Columbia Radiation Laboratory, Columbia University,  
New York, New York 10027

James L. Wilbur, John P. Folkers, and George M. Whitesides

Department of Chemistry, Harvard University, Cambridge, Massachusetts 02138

Received: November 30, 1994<sup>⊗</sup>

Scanning tunneling microscopy (STM) images of 1-docosanol, 1-docosanethiol, didocosyl disulfide, and 1-chlorooctadecane on graphite are compared. The images of the 1-docosanethiol and didocosyl disulfide show bright spots which are attributed to the positions of the S–H and S–S functional groups. The STM images of the 1-docosanol and 1-chlorooctadecane do not show such bright spots. The fact that both the S–H and S–S groups appear bright in the STM images indicates that the presence of an S atom on graphite results in a higher tunneling current when the tip scans over it compared to the tunneling current over a C, O, or Cl atom. The different behavior of the S atoms compared to the O, C, and Cl atoms is discussed in terms of the interactions between these atoms and the underlying graphite substrate. The persistent brightness of S atoms in the images of molecular adsorbates suggests that sulfur may serve as a useful “chromophore” for molecules imaged by STM.

### Introduction

By using the scanning tunneling microscope (STM) to image molecules adsorbed on a surface, the orientation of the adsorbate molecules relative to one another and the underlying substrate can be determined.<sup>1–3</sup> In addition, intermolecular interactions and the interaction between the adsorbed molecule and the surface can be studied.<sup>1–3</sup> While the STM can resolve individual molecules, the mechanism by which insulating molecules adsorbed on surfaces are imaged by the STM is still unclear. Typical bias voltages used while imaging molecules are far lower than the energy difference between the highest occupied molecular orbitals (HOMO) and the lowest unoccupied molecular orbital (LUMO) of the adsorbed molecules. Both experimental and theoretical work suggests that the STM images at these bias voltages do not correspond directly to the electronic structure of the adsorbed molecules but rather reflect perturbations of the solid substrate electronic states due to interactions between the surface and the adsorbed molecule.<sup>4–8</sup> Electronic structure calculations show that the interactions between the adsorbed molecule and the surface mix the substrate and molecular states (i.e., the substrate states are modified by the molecular states). Hence, the STM images reflect the symmetry of the surface but are “highlighted” by those regions of the surface where the solid substrate states are strongly modified due to the presence of the adsorbed molecule.<sup>7</sup>

This mixing of molecular and substrate states has been proposed to explain the STM images of liquid crystal molecules that contain both an aromatic ring and an aliphatic chain.<sup>5,6</sup> In these images, the aromatic rings appear much brighter than the aliphatic chains (i.e., the tunneling current over the aromatic rings is larger than that over the aliphatic chains). An alternate mechanism by which the STM might differentiate the aromatic rings from the aliphatic chains in these molecules is a modulation of the surface work function due to the presence of an adsorbed species.<sup>4</sup>

STM images of *n*-alcohols adsorbed on graphite indicate that the OH functional group cannot be distinguished from the methylene groups of the hydrocarbon chain attached to the OH group.<sup>1b,2,3</sup> On the other hand, much like the aromatic rings in liquid crystals described above,<sup>5,6</sup> sulfur atoms in the long chain molecule dihexadecyl disulfide have been reported to have enhanced conductivity compared to the alkyl chains when imaged on graphite.<sup>9</sup> In the experiments described here, we have investigated the effect of different functional groups (at the ends or the middle of hydrocarbon chains) on the tunneling current and, hence, the contrast over these functional groups as observed in the STM images. By comparing the contrast over a functional group to the contrast over the methylene groups that form the hydrocarbon chain, it should be possible to determine which functional groups can be readily distinguished by the STM (as was observed for aromatic rings in the images of liquid crystals and for sulfur atoms in long chain disulfides mentioned above). When the presence of different functional groups on a graphite substrate results in different tunneling currents as the tip scans over the surface, variations in the contrast (as observed in an STM image) can be used as a signature to identify functional groups and locate their positions within a molecule.

In this paper, we compare the STM images of alcohols (R–OH), alkanethiols (R–SH), alkyl chlorides (R–Cl), and alkyl disulfides (R–S–S–R). The alkanethiols were chosen as they are analogous to the alcohols, and they provide an opportunity to test for the presence of a general mechanism that produces bright images for sulfur atoms in the STM. The effect of the SH group on both the contrast and orientation of molecules observed in the STM images, as compared with the alcohols, has been studied. In order to determine the effect of increasing atomic size in a molecule on the contrast in the STM images, the alkyl chlorides are compared with the alkanethiols. The alkyl disulfides were investigated to provide a comparison with the thiols and to determine if placement of S atoms in different positions in the alkyl chains affected the STM images.

\* To whom all correspondence should be addressed.

<sup>⊗</sup> Abstract published in *Advance ACS Abstracts*, April 1, 1995.

## Experimental Section

Experiments were performed with a Digital Instruments Nanoscope III STM under ambient conditions. 1-Chlorooctadecane ( $\text{CH}_3(\text{CH}_2)_{17}\text{Cl}$ ) and 1-docosanol ( $\text{CH}_3(\text{CH}_2)_{21}\text{OH}$ ) were purchased from Aldrich and used without further purification. Solutions of approximately 1 mg/mL in phenyloctane (Aldrich) were prepared. Neat samples of 1-chlorooctadecane were used since it is a liquid at room temperature. The 1-docosanethiol ( $\text{CH}_3(\text{CH}_2)_{21}\text{SH}$ ) and didocosyl disulfide ( $\text{CH}_3(\text{CH}_2)_{21}-\text{S}-\text{S}-\text{CH}_3(\text{CH}_2)_{21}$ ) were synthesized as described previously.<sup>10</sup> The alkanethiols oxidize in air to form the disulfides ( $\text{R}-\text{S}-\text{S}-\text{R}$ ,  $\text{R} = \text{C}_{22}\text{H}_{45}$ ). To slow the rate of oxidation so that the STM images obtained were those of the alkanethiols and not the disulfides, we removed oxygen dissolved in the solvent (phenyloctane) by bubbling argon or nitrogen through the solvent, for about 15–20 min, before dissolving the alkanethiols. Solutions of approximately 1 mg/mL in phenyloctane were prepared for both docosanethiol and didocosyl disulfide. A drop of solution was deposited on a piece of freshly cleaved highly ordered pyrolytic graphite (HOPG), purchased from Advanced Ceramics Corporation. The STM tips used were 0.01 in. diameter Pt/Rh (87/13) wire that were snipped with wire cutters. The tip was immersed in solution and the STM images obtained under a liquid drop. Typical tunneling conditions were 1200–1600 mV and 100–160 pA with the STM operating either in the constant current or constant height modes. The images of thiols and disulfides were obtained with the sample biased either positive or negative with respect to the tip, while images of alcohols and chlorides were obtained with the sample biased negative with respect to the tip. The scan rates varied depending on the size of the area being imaged and on the mode of operation. Images were obtained with different tips and samples to check for reproducibility and to ensure that the images were free from artifacts caused by the tip or sample.

## Results

An STM image of docosanethiol on graphite is shown in Figure 1. The most striking feature is the presence of bright spots dispersed over the image. Visible at lower contrast are bands connected to these bright spots. The length of these bands agrees well with the length of a  $\text{C}_{22}$  carbon chain indicating that these bands correspond to the  $\text{C}_{22}$  alkyl chains oriented parallel to the graphite surface. (On gold, by contrast, alkanethiolates are chemisorbed on the surface through a  $\text{S}-\text{Au}$  bond, and the alkyl chains orient at an angle  $30^\circ$  from the normal to the gold surface.<sup>11</sup>) The parallel orientation of the alkanethiols on graphite suggests that they are physisorbed on the graphite surface. In addition, the alkanethiols appear to desorb readily from the surface and to go back into solution. This desorption can be observed by monitoring, with the STM, an area of the surface as a function of time. In these images the orientation of the molecular rows varies on a time scale of the order of a few minutes to tens of minutes with loss of resolution occurring during this reorientation. We hypothesize that the reorientation of molecular rows is due to molecules desorbing off the surface and going back into solution. This molecular motion results in a loss of resolution in the STM images. Molecules in solution can then readsorb onto the bare surface forming rows with different orientations on the graphite. Once a "new" layer of molecules is formed, the STM is again able to image these molecules. The fact that the molecules appear to desorb readily from the surface suggests that they are not bound covalently to the graphite.

On close inspection of the alkanethiol images, each bright spot can be assigned to an alkyl chain, and whenever one end

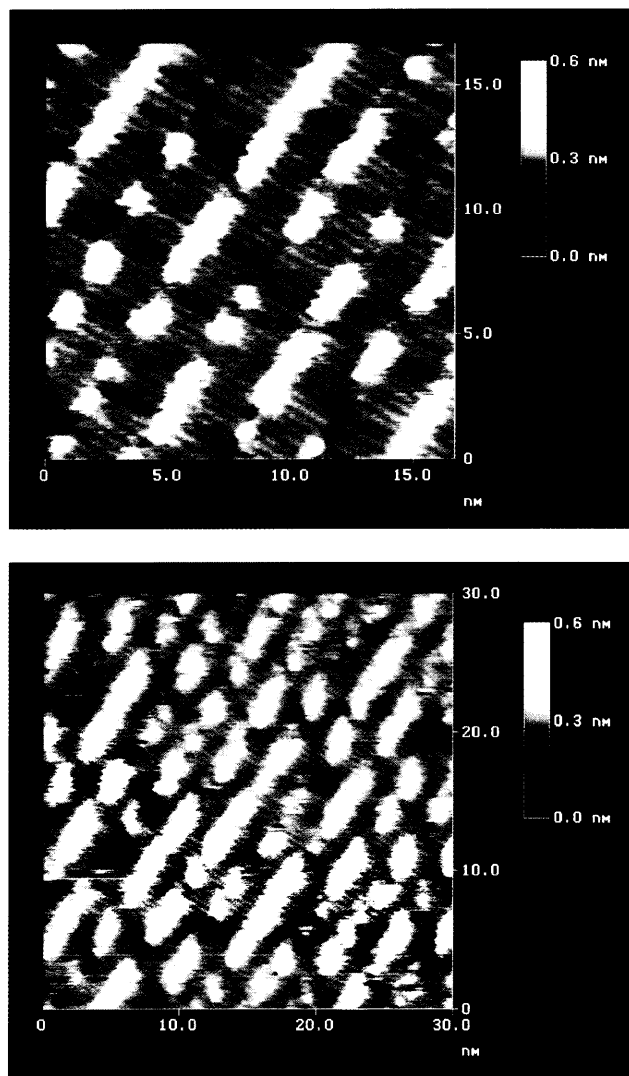


**Figure 1.** STM image of 1-docosanethiol ( $\text{CH}_3(\text{CH}_2)_{21}\text{SH}$ ) in phenyloctane adsorbed on graphite. (a, top) A  $15\text{ nm} \times 15\text{ nm}$  image of the alkanethiol molecules. The bright spots dispersed over the image are attributed to the SH functional groups, and the bands at lower contrast connected to each bright spot are the alkyl chains. The angle between the molecular axis and the troughs between two rows is  $90^\circ$ . (b, bottom) A  $30\text{ nm} \times 30\text{ nm}$  image which shows the random distribution of the bright spots corresponding to the positions on the SH groups. Tunneling conditions were 1550 mV (sample positive) and 150 pA in the constant current mode.

of an alkyl chain has a bright spot, the other end is dark. These bright spots are attributed to the thiol (SH) functional group at the end of the  $\text{C}_{22}$  carbon chain. From the STM images, it appears that some of the alkanethiols are arranged such that the SH groups of molecules in adjacent rows face each other (i.e. head-to-head); for other regions of the image, the  $\text{CH}_3$  end of a molecule in one row faces the thiol end of a molecule in the adjacent row (head-to-tail). The angle between the molecular axis and a line drawn along the troughs between two rows is  $90^\circ$ . On a few occasions domain formation was observed over the regions being imaged. The rows of alkanethiols in one domain are oriented at  $120^\circ$  with respect to the rows in the neighboring domain. Within a domain the rows of alkanethiols form straight lines. The images of the alkanethiols were the same whether the sample was biased positive or negative with respect to the tip. The contrast observed along a molecule did not depend on the polarity of the bias voltage applied to the sample.

Since the S atoms in long chain disulfides have been reported to show enhanced STM contrast,<sup>9</sup> it is possible that the STM

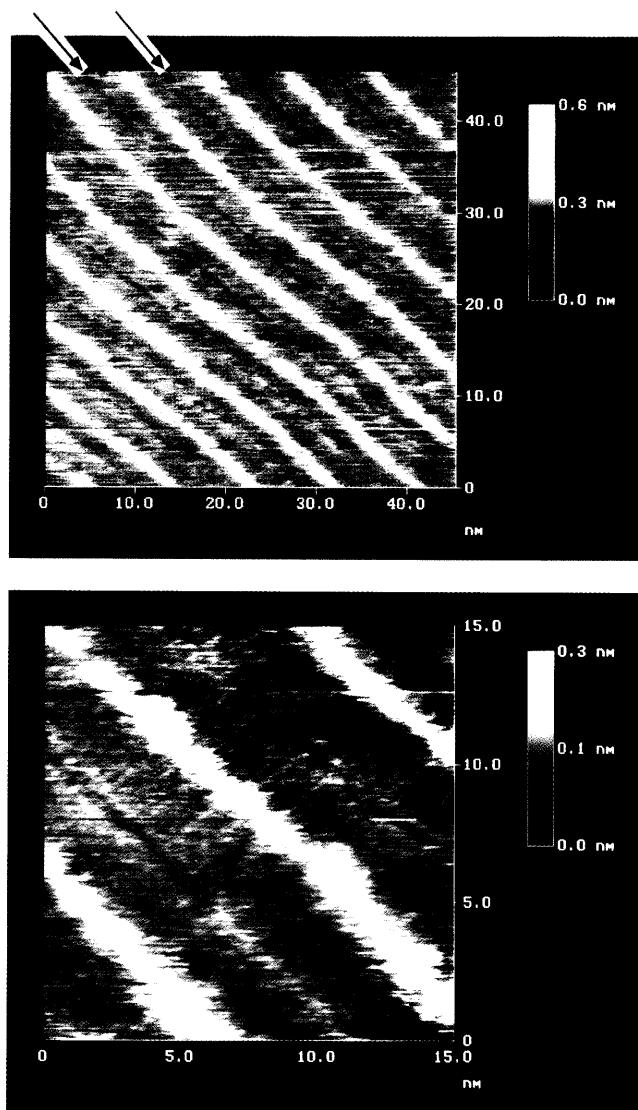


**Figure 2.** STM image of didocosyl disulfide ( $\text{CH}_3(\text{CH}_2)_{21}-\text{S}-\text{S}-(\text{CH}_2)_{21}\text{CH}_3$ ) in phenyloctane adsorbed on graphite. (a, top) A  $45 \text{ nm} \times 45 \text{ nm}$  image of the disulfides showing rows of bright spots alternating with dark rows. The bright rows are due to the S-S groups, and the dark rows (indicated by the arrows) are the  $\text{CH}_3$  ends of the alkyl chains. Tunneling conditions were  $-1350 \text{ mV}$  (sample negative) and  $110 \text{ pA}$  in the constant current mode. (b, bottom) A  $15 \text{ nm} \times 15 \text{ nm}$  image of the disulfides. Tunneling conditions were  $-1350 \text{ mV}$  (sample negative) and  $130 \text{ pA}$  in the constant current mode.

images of the alkanethiols (of the type shown in Figure 1) are not those of the alkanethiols but of alkyl disulfides ( $\text{R}-\text{S}-\text{S}-\text{R}$ ,  $\text{R} = \text{C}_{22}$ ) formed by the oxidation of the alkanethiols. In these experiments the solvents used were first purged with argon or nitrogen in order to displace dissolved oxygen. The STM images were, however, obtained in air, and it is, therefore, possible that during the process of imaging the molecules in solution undergo oxidation. In order to investigate this hypothesis further, STM images of didocosyl disulfide,  $\text{CH}_3(\text{CH}_2)_{21}-\text{S}-\text{S}-(\text{CH}_2)_{21}\text{CH}_3$ , were obtained. Figure 2a is an STM image of a  $45 \text{ nm} \times 45 \text{ nm}$  area of didocosyl disulfide on graphite. As in the images of the alkanethiols, the images of the disulfides reveal bright spots much like those observed for dihexadecyl disulfide,<sup>9</sup> indicating that the tunneling current over the S-S group is larger than that over the hydrocarbon chain. This difference in contrast marks the position of the S-S group in a molecule (see Figure 2b). Unlike the images of the alkanethiols, which reveal an apparently *random* distribution of bright spots, the images of the alkyl disulfides show highly ordered

bright spots that lie along the same line indicating that the S-S groups of molecules within the same row lie along the same line.

As can be seen from the images in Figure 2, the pattern of contrast in these images is a bright row (corresponding to the S-S groups), followed by a dark row. The dark rows in the images of the disulfides correspond to the  $\text{CH}_3$  ends of the molecules and the distance between any two dark rows agrees with the length of two  $\text{C}_{22}$  alkyl chains, i.e., the length of a  $\text{CH}_3(\text{CH}_2)_{21}-\text{S}-\text{S}-(\text{CH}_2)_{21}\text{CH}_3$  molecule. On comparing the images of the alkanethiols and disulfides, it appears that for the alkanethiols, when the bright spots appear in adjacent rows (where the distance between these bright spots corresponds to the length of only one  $\text{C}_{22}$  chain) the molecules imaged are the alkanethiols; if the bright spots appear in alternate rows (where the distance between these bright spots corresponds to the length of two  $\text{C}_{22}$  chains), the molecules imaged could either be the alkanethiols (tail-to-tail) or a disulfide oxidation product. Therefore, it is possible that the images of the alkanethiols could have some contribution from disulfide impurities; nevertheless, the S atoms in the S-H functional group, like their counterparts in the disulfide chains shown here in Figure 2 and reported earlier,<sup>9</sup> clearly reveal enhanced contrast when compared to the alkyl chains. Since the images of both the disulfides and alkanethiols reveal a higher tunneling current over the S-H and S-S groups than over the rest of the molecule, it is evident that S atoms on graphite produce a very different tunneling current when the STM tip scans over them than when the tip scans over C atoms.

Figure 3a shows an STM image of 1-chlorooctadecane on graphite. Unlike the images of the alkanethiols and alkyl disulfides, the images of the chlorooctadecane indicate that the contrast of the chain ends and the rest of the molecule are the same. Therefore, it is not possible to determine at which end of the hydrocarbon chain the chlorine atom is located. As with the thiols, the angle between the molecular axis and a line drawn along the troughs between two rows is  $90^\circ$ , and the rows of molecules form straight lines on the graphite surface.

STM images of alcohols have been observed previously.<sup>1b,2,3</sup> An STM image of 1-docosanol on graphite is shown in Figure 3b. From the STM images of alcohols it is not possible to determine at which end of the chain the OH group is located. However, as opposed to the  $90^\circ$  orientation of the alkyl chains of the thiols and the chlorides with respect to the line separating the rows, the angle between the molecular axis and a line drawn along the troughs between two rows is  $60^\circ$  for the alcohol molecules.

## Discussion

As can be seen from the STM images of the four molecules shown in Figures 1–3, the thiols and disulfides behave quite differently from alcohols and alkyl chlorides. The STM clearly distinguishes the S atom from the C atoms in the alkyl chains as evidenced by the bright spots in the images of these molecules. Because of this unexpectedly high contrast for the sulfur atoms, the position of the S-H or S-S functional group in these molecules can be located unambiguously; this type of atom-specific location is not possible for the alcohols and the alkyl chlorides. The bright spots indicate that the tunneling current over an S atom is substantially larger than that over a C, Cl, or O atom.

From the locations of the bright spots in the alkanethiol images, it appears that the alkanethiol molecules in a row are oriented such that not all the SH groups lie on the same line. Also, the SH group of a molecule in one row does not

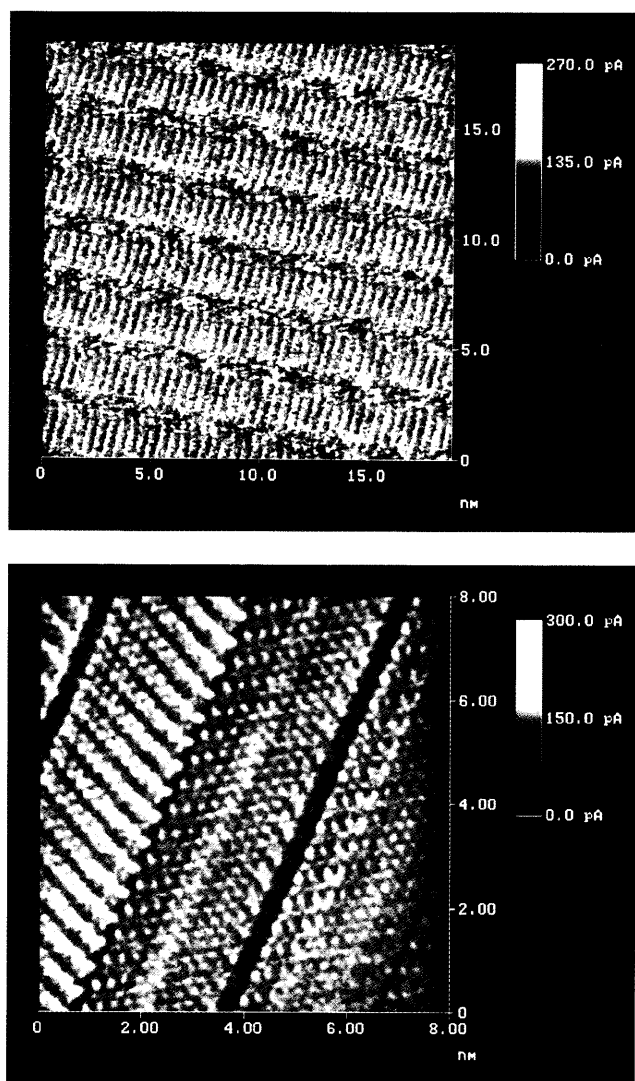


**Figure 3.** (a, top) An STM image of 1-chlorooctadecane ( $\text{CH}_3(\text{CH}_2)_{17}\text{-Cl}$ ) adsorbed on graphite. Unlike the images of the alkanethiols, the position of a Cl atom in a molecule cannot be determined. The angle between the molecular axis and the troughs between two rows is  $90^\circ$ . Tunneling conditions were  $-1500$  mV (sample negative) and  $120$  pA in the constant height mode. (The image has been low-pass filtered). (b, bottom) An STM image of 1-docosanol ( $\text{CH}_3(\text{CH}_2)_{21}\text{OH}$ ) in phenyloctane adsorbed on graphite. As with the alkyl chlorides, the position of the OH group in this molecule cannot be determined. For the alcohols, however, the angle between the molecular axis and the troughs between two rows is  $60^\circ$ . Tunneling conditions were  $-1300$  mV (sample negative) and  $85$  pA in the constant current mode. (The image has been low-pass filtered).

necessarily face that of an SH group of a molecule in the adjacent row. This orientational disorder of SH and  $\text{CH}_3$  groups is quite different from the packing of the alcohols on graphite where all the OH groups of molecules in one row lie on the same line, and the OH groups of molecules in adjacent rows face one other so as to hydrogen bond to each other.<sup>1b,2,3</sup> For the alcohols, hydrogen bonding between molecules plays a major role in determining the long and short range order of these molecules on graphite.<sup>1b,2,3</sup> The formation of a network of hydrogen bonds between the alcohol molecules also helps to stabilize this species on the surface.

The fact that the alkanethiols are not all aligned with neighboring SH groups facing each other suggests that hydrogen bonding between the SH groups does not dominate the stabilization of these molecules on the surface. In fact, it is quite likely that the thiols are not hydrogen bonded to each other. The SH group is known to be a weak proton donor; thiol (SH) groups

do not form hydrogen bonds or form hydrogen bonds only with strong bases (e.g. nitrogen bases like pyridine).<sup>12</sup> In the case of the alkanethiols on graphite, stabilization appears to be due primarily to lateral interactions between molecules in a row. This mode of stabilization is similar to that of alkanes on graphite<sup>1a,2a,3</sup> where the orientation of molecules in a row is analogous to that for the alkanethiols. The lateral interactions between molecules is clearly also important for stabilizing the alkyl chlorides on the graphite surface, since these molecules also adopt a  $90^\circ$  orientation with respect to the troughs between two rows.

In the images of dialkyl disulfides shown in Figure 2 and reported earlier,<sup>9</sup> the bright spots corresponding to the S-S groups lie along the same line. This ordering of the S-S groups differs from the disorder of the SH groups in the alkanethiol images, where the bright spots (corresponding to the SH groups) appear to be more randomly distributed over the area imaged. For the disulfides lateral interactions between the alkyl chains of the molecules are probably the dominant intermolecular interactions. These interactions will be optimized if the molecules within a row are aligned such that the S-S groups lie along the same line, thus ensuring overlap between the alkyl chains of adjacent molecules. For the alkanethiols, the overlap between alkyl chains does not depend on the alignment of SH groups of molecules in the same row, resulting in the more random distribution of bright spots in these images. The C-S-S-C dihedral angle in dialkyl disulfides is strongly favored at  $90^\circ$ ; the value that is adopted in the surface-adsorbed species is not *a priori* clear,<sup>13</sup> but V shaped structures have been reported for dihexadecyl disulfide on HOPG.<sup>9</sup>

The large tunneling current measured over the S atom in the alkanethiols and dialkyl disulfides is similar to that observed for STM images of liquid crystal molecules containing aromatic rings on graphite. In the liquid crystal images, the aromatic rings appear much brighter than the alkyl chains attached to the rings.<sup>4-6</sup> Different explanations for the bright aromatic ring images have been proposed. Spong et al. suggested that the difference between the intensities of the aromatic rings and the alkyl chains in the STM images is due to the difference in their molecular polarizabilities.<sup>4</sup> The work function of a bare surface can be changed by the presence of an adsorbed molecule through the molecular polarizability.<sup>4,14</sup> Variations in the polarizability along a molecule will, therefore, result in variations of the surface work function under the molecule. Since the tunneling current depends on the work function,<sup>15</sup> the STM images reflect spatial variations in the work function of the surface due to the presence of adsorbed molecules. Because the polarizability of an aromatic ring is larger than that of the alkyl chain, the work function of the surface under the aromatic ring will be more strongly altered than the work function of the surface under the alkyl chain. Therefore, as the STM tip moves across the surface, it would measure a different tunneling current over an aromatic group than over an alkyl chain.

Another explanation given for the difference in the contrast between the aromatic rings and the alkyl chains in liquid crystal molecules is the increase in the local density of states (LDOS) near the Fermi level of the surface due to mixing of molecular and substrate states.<sup>5-7</sup> Since the tunneling current depends on the LDOS near the Fermi level of the surface,<sup>15</sup> any change in this density will result in a change in the tunneling current. In the case of molecules adsorbed on a surface, interactions between the molecule and the surface result in a mixing of the molecular states with the surface states. Theoretical calculations indicate that at typical bias voltages used in STM experiments, even though the molecular states are not resonant with the

**TABLE 1: Atomic Polarizabilities of Oxygen, Sulfur, Chlorine, and Hydrogen Relative to That of Carbon (Values Obtained from Ref 17)**

atomic polarizability				
carbon	oxygen	sulfur	chlorine	hydrogen
1.00	0.45	1.65	1.24	0.38

energy of the tunneling electrons, there is a sufficient change in the LDOS to cause the tunneling current to be different from that of the bare surface.<sup>7,16</sup> In order to explain why the aromatic rings in the liquid crystal molecules appear bright in the STM images, it has been suggested that the molecular orbitals of the aromatic rings contribute sufficiently to increase the LDOS near the Fermi level of the surface. Therefore, the tunneling current over these groups is larger than that over the rest of the molecule, and the aromatic rings appear bright in the STM images.

While the details of the above mechanisms differ, they both emphasize the fact that the magnitude of the tunneling current depends on the extent to which the underlying surface is modified by the presence of the adsorbed species. The perturbation caused by the interaction between the surface and the adsorbed molecules affects the spatial distribution of both the work function and the wave function of the surface. Therefore, if different parts of a molecule perturb these surface properties differently, the tunneling current over the molecule will vary as the tip moves across the molecule. The STM images, therefore, correspond to features of the surface modulated by the presence of the adsorbed species.

The difference between images of alkanethiols and alcohols may result from the difference in the number of electrons in a sulfur or oxygen atom; sulfur has twice as many electrons as oxygen. Since the STM measures variation in electron density as the tip rasters across the surface, variations in the number of electrons between atoms could result in different tunneling currents over different atoms. If, however, the tunneling current depends only on the number of electrons in a molecule, then STM images of alkyl chlorides should also show a bright spot corresponding to the position of the chlorine atoms (since chlorine has one more electron than sulfur). The lack of bright spots in the images of chlorooctadecane (Figure 3a) indicates that the tunneling current over a chlorine atom is not larger (or even comparable) to the tunneling current over a sulfur atom. This observation suggests that the number of electrons in an atom does not determine directly the magnitude of the tunneling current.

The differences between images of the thiols, disulfides, alcohols, and chlorides could be due to the difference in the strength of the interactions between these functional groups and the graphite substrate. A stronger interaction between an atom (or a group of atoms) and the substrate could result in a larger perturbation of both the work function and the wave function of the surface under this atom (or group of atoms) and, hence, a different tunneling current over this region. The strength of the interaction between S, O, C, Cl, and H atoms and the substrate may vary with their atomic polarizabilities, since a more polarizable atom is expected to interact more strongly with the substrate. Table 1 lists the atomic polarizabilities of sulfur, oxygen, chlorine, and hydrogen relative to that of a carbon atom;<sup>17</sup> the atomic polarizability of a sulfur atom is larger than that of a carbon atom; the polarizability of a chlorine atom is close to that of a carbon atom; the polarizability of an oxygen atom is about half that of a carbon atom; and the polarizability of a hydrogen atom is much smaller than that of a carbon atom. If the interactions between the adsorbed molecules and the surface depend primarily on the polarizability, then the sulfur

atom would have the strongest interaction with the graphite surface, followed by chlorine, carbon, oxygen, and hydrogen, respectively, resulting in an increased tunneling current when the tip scans over the S-H and S-S functional groups relative to all other functional groups studied here. If the S atoms protrude from the surface significantly compared to the other atoms in the adsorbate chain and tunneling occurs directly to the adsorbate (as opposed to the graphite surface), the S atoms would also appear bright in the image. This, however, seems to be an unlikely explanation given the large polarizability of the S atoms, which suggests a strong attractive interaction with the surface.

If the change in the polarizability across a molecule determines the STM contrast, the images of the alkyl chloride might be expected to show a slight increase in intensity for the chlorine atoms relative to the carbon chain since the polarizability of Cl is slightly larger than that of C. The STM images of the alkyl chloride, however, do not show any enhancement in the tunneling current over the ends of the molecules. The value of the polarizability of the Cl atom may not be sufficiently different from that of the C atom to cause a significant difference in the perturbations of the graphite electronic structure.

In addition to the perturbation of the graphite substrate by the adsorbate molecule, it is possible that the tunneling tip interacts with the adsorbate molecule. The tunneling current between the tip and sample depends on the density of states at the Fermi level of the tip (as well as that of the surface).<sup>18</sup> Interactions between the tunneling tip and sample molecule may change the density of states at the Fermi level of the tip. If the strength of the interaction between the tunneling tip and an atom depends on the nature of the atom, then the tunneling current may also vary as the tip scans over different atoms. (Indeed, electron scattering quantum chemical calculations have been used to show that the tunneling current over sulfur atoms adsorbed on Re(0001) is a sensitive function of whether a sulfur or a rhenium atom terminates the tip.<sup>16f</sup> It is possible that the higher tunneling current measured as the tip scans over an S atom, relative to that near a C, O, or Cl atom, is the result of a stronger interaction between an S atom in the adsorbate molecule and the tunneling tip. STM experiments have demonstrated that tip-sample interactions are important in moving atoms and molecules on a surface with the tunneling tip.<sup>19-21</sup> Moving an atom on the surface, however, requires tunneling conditions (low bias voltage and high tunneling currents) where the tip is close to the surface and in contact with the atom to be moved. The images shown in Figures 1-3 were obtained at high bias voltages (~1300-1500 mV) and low tunneling currents (~85-150 pA). With these tunneling conditions the tunneling tip is relatively far from the surface. While tip-sample interactions cannot be ruled out completely, it is unlikely that they would be strong enough at these separations to explain the high tunneling current observed as the tip scans over an S atom in an alkanethiol or dialkyl disulfide molecule.

Using a jellium model Lang has found that the higher energy portion of the state density spectrum for a single adatom on a metal surface is reflected in the apparent vertical size of the adatom as a function of bias.<sup>16c</sup> Interestingly, this study predicts a lowering of the tunnel current over a single sulfur atom because the sulfur pushes some of the metal state density away from the region of the surface where the single sulfur atom sits. This is, of course, the opposite of what is observed here for sulfur covalently bound in a molecular adsorbate sitting on graphite, indicating, not surprisingly, that the details of the adsorbate and/or conducting substrate electronic structure are quite critical in determining the nature of the STM images for

these weakly coupled surface—adsorbate systems. Many body, electron screening effects have also been suggested as a source of the coupling of adsorbate and substrate surface electronic states, a further indication of the sensitivity of the tunneling process to the detailed electronic structure of the species involved.<sup>16e</sup>

One other possible origin of the bright sulfur atom images is the formation of an adsorbate negative ion.<sup>22,23</sup> If such a species can be formed in these experiments, it might well provide a facile low-energy path for tunneling between the tip and the graphite surface. The formation of a transient adsorbate negative ion as an intermediate in the process of tunneling from tip to surface cannot be ruled out at this time and remains an active area of investigation.

## Conclusions

STM images of alkanethiols under phenyloctane solvent on graphite indicate that the tunneling current near the thiol functional group is much larger than that of the methylene groups in the hydrocarbon chain. This contrast allows us to identify and locate the position of the thiol functional group in a molecule adsorbed on a surface. Images of the dialkyl disulfides, for both didocosyl disulfide studied here and for dihexadecyl disulfide investigated earlier,<sup>9</sup> also reveal bright spots corresponding to the position of the S—S groups. For alkyl chlorides and alcohols on graphite, however, the tunneling current of the chlorine and OH groups is similar to that of the methylene groups of the hydrocarbon chain. Hence, it is not possible to identify directly the position of these functional groups in a molecule from the STM contrast. Of the atoms in the different functional groups investigated here, the S atom has the largest atomic polarizability. It is possible that the larger polarizability of the S atom may result in a stronger interaction with the surface, which can have an effect on both the work function and the wave function of the surface, leading to a brighter image for the sulfur. If the high contrast of sulfur in these images is a general phenomenon, thiols, disulfides, and other sulfur-containing species may be useful “chromophores” for imaging by STM.

**Acknowledgment.** Work at Columbia was supported by The Joint Services Electronics Program (U.S. Army, Navy and Air Force; DAAHO4-94-40057), the Donors of the Petroleum Research Fund administered by the American Chemical Society, and the National Institute of Health (1 R03 RR06987-01A1). Equipment support was provided by the National Science Foundation (CHE-91-18782). Work at Harvard was supported

in part by ARPA and by the Office of Naval Research. J.L.W. gratefully acknowledges an NIH Postdoctoral Fellowship.

## References and Notes

- (1) (a) McGonigal, G. C.; Bernhardt, R. H.; Thomson, D. J. *Appl. Phys. Lett.* **1990**, *57*, 28. (b) McGonigal, G. C.; Bernhardt, R. H.; Yeo, Y. H.; Thomson, D. J. *J. Vac. Sci. Technol.* **1991**, *B9*, 1107.
- (2) (a) Rabe, J. P.; Buchholz, S. *Science* **1991**, *253*, 424. (b) Buchholz, S.; Rabe, J. P. *Angew. Chem., Int. Ed. Engl.* **1992**, *31*, 189.
- (3) Venkataraman, B.; Breen, J. J.; Flynn, G. W. *J. Phys. Chem.* **1995**, *99*, 6608.
- (4) Spong, J. K.; Mizes, H. A.; LaComb, L. J., Jr.; Dovek, M. M.; Frommer, J. E.; Foster, J. S. *Nature* **1989**, *338*, 137.
- (5) Nejoh, H. *Appl. Phys. Lett.* **1990**, *57*, 2907.
- (6) Smith, D. P. E.; Hörber, J. K. H.; Binnig, G.; Nejoh, H. *Nature* **1990**, *344*, 641.
- (7) Fisher, A. J.; Blöchl, P. E. *Phys. Rev. Lett.* **1993**, *70*, 3263.
- (8) Hallmark, V. M.; Chiang, S. *Phys. Rev. Lett.* **1993**, *70*, 3740.
- (9) Rabe, J. P.; Buchholz, S.; Askadskaya, L. *Synth. Met.* **1993**, *54*, 339.
- (10) Bain, C. D.; Troughton, E. B.; Tao, Y.-T.; Evall, J.; Whitesides, G. M.; Nuzzo, R. G. *J. Am. Chem. Soc.* **1989**, *111*, 321.
- (11) (a) Porter, M. D.; Bright, T. B.; Allara, D. L.; Chidsey, C. E. D. *J. Am. Chem. Soc.* **1987**, *109*, 3559. (b) Laibinis, P. E.; Whitesides, G. M.; Allara, D. L.; Tao, Y.-T.; Parikh, A. N.; Nuzzo, R. G. *J. Am. Chem. Soc.* **1991**, *113*, 7152. (c) Dubois, L. H.; Nuzzo, R. G. *Annu. Rev. Phys. Chem.* **1992**, *43*, 437.
- (12) Pimentel, G. C.; McClellan, A. L. *The Hydrogen Bond*; W. H. Freeman and Company: San Francisco and London, 1960; p 201.
- (13) Singh, R.; Whitesides, G. M. In *Sulfur-Containing Functional Groups: Supplement S*; Patai, S., Ed.; John Wiley and Sons: New York, 1993; Chapter 13.
- (14) Antoniewicz, P. R. *Surf. Sci.* **1975**, *52*, 703.
- (15) Tersoff, J.; Hamann, D. R. *Phys. Rev.* **1985**, *B31*, 805.
- (16) (a) Eigler, D. M.; Weiss, P. S.; Schweizer, E. K.; Lang, N. D. *Phys. Rev. Lett.* **1991**, *66*, 1189. (b) Lang, N. D. *Phys. Rev. Lett.* **1986**, *56*, 1164. (c) Lang, N. D. *Phys. Rev. Lett.* **1986**, *58*, 45. (d) Lang, N. D. *Phys. Rev.* **1988**, *B37*, 10395. (e) Mintmire, J. W.; Harrison, J. A.; Colton, R. J.; White, C. T. *J. Vac. Sci. Technol.* **1992**, *A10*, 603. (f) Dunphy, J. C.; Ogletree, D. F.; Salmeron, M. B.; Sautet, P.; Bocquet, M.-L.; Joachim, C. *Ultramicroscopy* **1992**, *42–44*, 490.
- (17) *Handbook of Chemistry and Physics*, 73rd ed.; CRC Press, Inc.: Boca Raton, FL, 1992–1993; pp 10–197.
- (18) Hamers, R. J. *Annu. Rev. Phys. Chem.* **1989**, *40*, 531.
- (19) Foster, J. S.; Frommer, J. E.; Arnett, P. C. *Nature* **1988**, *331*, 324.
- (20) (a) Eigler, D. M.; Schweizer, E. K. *Nature* **1990**, *344*, 524. (b) Eigler, D. M.; Lutz, C. P.; Rudge, W. E. *Nature* **1991**, *352*, 600. (c) Stroscio, J. A.; Eigler, D. M. *Science* **1991**, *254*, 1319.
- (21) (a) Lyo, I.-W.; Avouris, P. *Science* **1991**, *253*, 173. (b) Hasegawa, Y.; Avouris, P. *Science* **1992**, *258*, 1763.
- (22) (a) Engelking, P. C.; Ellison, G. B.; Lineberger, W. C. *J. Chem. Phys.* **1978**, *69*, 1826. (b) Cremonini, M. A.; Lunazzi, L.; Placucci, G. *J. Chem. Soc., Perkin Trans. 2* **1992**, *2*, 321.
- (23) (a) Brinkman, E. A.; Gunther, E.; Schafer, O.; Brauman, J. I. *J. Chem. Phys.* **1994**, *100*, 1840. (b) Jordan, K. D.; Burrow, P. D. *Acc. Chem. Res.* **1978**, *11*, 341.

JP943168D